Polymer 43 (2002) 7325–7333

polymer

www.elsevier.com/locate/polymer

Epoxy-based azo polymers: synthesis, characterization and photoinduced surface-relief-gratings

Yaning He, Xiaogong Wang*, Qixiang Zhou

Department of Chemical Engineering, Tsinghua University, Beijing 100084, People's Republic of China

Received 27 June 2002; received in revised form 3 September 2002; accepted 13 September 2002

Abstract

Epoxy-based azo polymers with three kinds of backbones, different types of azo chromophores, and selected degrees of functionalization (DFs), were synthesized through a post-polymerization azo-coupling scheme. The T_gs of the azo polymers were found to be considerably influenced by the substituents on the 4-positions of the azobenzene units and increased with the increase of the DFs of the polymers. Surface-relief-gratings (SRGs) were induced on the polymer films by interferenced Ar^+ laser beams. With the same irradiating light intensity and approximately equal film thickness, the rates of SRG formation were found to be significantly dependent on the electron-withdrawing groups on the 4-positions of the azobenzene units. For the polymers with the same type of azo chromophores and backbone structure, the inscription rates increased with the increase of the DFs. Meanwhile, the backbone structure also exhibited some effect on the inscription rates through the ways such as changing chromophore loading density or main-chain rigidity. © 2002 Elsevier Science Ltd. All rights reserved.

Keywords: Azo polymers; Inscription rate; Surface-relief-gratings

1. Introduction

In recent years, polymers containing aromatic azo chromophores, also named as azo polymers, have been extensively investigated for scientific interest and potential applications in various photonic devices [1–6]. Recently, it has been reported that large surface modulations can be reversibly photoinduced on surfaces of azo polymer films [7–9]. The photoinduced surface-relief-gratings (SRGs) are formed upon exposure to an interference pattern of Ar^+ laser beams at modest intensities [7–14]. The surface relief structures formed are stable below the glass transition temperatures (T_gs) of the polymers and can be removed by heating samples to their T_gs or erased optically even below the T_gs [12–14]. It has been well documented that the inscription-erasure process is highly reproducible and not related with a permanent damage such as photodegradation or laser ablation [7–14]. Complex surface patterns can be easily produced by selecting suitable photofabrication conditions [15,16]. The method to reversibly photofabricate various surface structures could be very useful in many future applications [15–18].

The forming mechanism of the photofabricated SRGs has been actively investigated [7–14,19–26]. It is generally accepted that the SRGs are formed due to large-scale migration of the polymer chains induced by the low power laser irradiation and the photoinduced *trans–cis–trans* isomerization cycles of the azo chromophores play a key role in the process [7–14]. However, the understanding of the exact relationship between the cis–trans isomerization and the mass transport is still evolving [19–26]. The large-scale mass transport of the polymer chains has been attributed to internal pressure gradients produced by an isomerization-driven free volume expansion [19], anisotropic intermolecular interactions resulted from photoinduced ordering of dye molecules [20], worm-like movement in a direction parallel to former orientation of the azo molecules [21], dipole interaction of azo chromophores with the electric field gradient present in the polymer materials [22].

In order to fully understand this novel photoinduced dynamic process of azo polymers, an intensive study on the correlation between the polymer structure and the SRG formation properties is required. The photoinduced dynamic process can be affected by a few structural factors of azo

---

* Corresponding author. Tel.: +86-10-62784561; fax: +86-10-62770304.

E-mail address: wxg-dce@mail.tsinghua.edu.cn (X. Wang).

PII: S0032-3861(02)00644-4

polymers such as chemical structure of backbones, types of azo chromophores, positions to which azo chromophores are attached, and degree of functionalization among others. The formation of SRGs has been studied for types of side-chain azo polymers such as epoxy-based polymers, polyacrylates, polyesters, and polydiacetylenes [7–13,27–29]. Main-chain azo polymers have also been explored for SRG fabrication [30,31]. The effect of three kinds of azo chromophores linked to a polyacrylate or a polymethacrylate backbone has been investigated by Barrett et al. [12], it was found that the most bulky azo chromophore induces the SRG with the highest efficiency. Fukuda et al. [32] have reported the dependence of SRG formation rates on the degree of functionalization of the azo chromophores. Most recently, differences in the SRG fabrications concerning the formation of peaks or valleys in the illuminated areas have been reported to be related with the substituents on azobenzene units [27].

In this study, several novel types of epoxy-based azo polymers have been synthesized through a post-polymerization azo-coupling scheme. The post-polymerization azo-coupling scheme has been used to prepare nonlinear optical azo polymers by introducing various azo chromophores through the azo-coupling reaction between precursor polymers and diazonium salts at the final stage of the polymer synthesis [33,34]. The reaction route can provide a convenient and often the simplest way to synthesize side-chain azo polymers containing various types of azo chromophores, which generally has high reaction yields and can reach high degrees of functionalization (DFs) [33,34]. For studying the structure–property relationship, following advantages for this synthetic route can be expected. The DFs of the obtained polymers can be controlled quantitatively by selecting suitable feed ratios between the diazonium salts and the reactive aniline moieties of the precursor polymers. As the post-functionalization can be carried out on the same batch of the precursor polymers, the polymerization degrees of each series of azo polymers to be studied are the same. In this study, the azo polymers with three kinds of backbones, containing different types of azo chromophores and functionalized to different degrees, have been synthesized and carefully characterized. The structure–property relation of the polymers has been studied through SRG inscription experiments. The effect of backbones, substituents, and DFs on the inscription rates and saturation levels of these polymers for the SRG formation have been studied and discussed in detail.

2. Experimental

2.1. Characterization

The IR spectra were determined using a Nicolet 560-IR FT-IR spectrometer by incorporating samples in KBr disks. The ^{1}H NMR spectra were obtained on a Bruker-500 (500 MHz for proton) FT-NMR spectrometer. The UV–vis spectra of the samples were recorded by a Perkin–Elmer Lambda Bio-40 spectrometer. The thermal properties of the polymers were investigated with TA instrument DSC 2910 at a heating rate of 10 °C/min. The molecular weights of the polymers and their distributions were determined by gel permeation chromatography (GPC) utilizing a Waters model 515 pump and a model 2410 differential refractometer with three styragel columns HT2, HT3, HT4 connected in a serial fashion. THF was used as the eluent at a flow rate of 1.0 ml/min. Polystyrene standards with dispersity of 1.08–1.12 obtained from Waters were employed to calibrate the instrument.

2.2. Materials

4,4′-Bis(2,3-epoxypropoxy)diphenyl and 1,4-bis(2,3-epoxypropoxy)benzene were synthesized by the reaction of 4,4′-dihydroxydiphenyl or 1,4-dihydroxybenzene with epichlorohydrin according to the literature [35]. Diglycidyl ether of bisphenol-A ($M_w = 392$) was purchased as a commercial product from Shell Company. All other reagents and solvents were used as received without further purification.

2.3. Polymer synthesis

BP–AN: BP–AN was obtained from the reaction between diglycidyl ether of bisphenol-A (32.7 g, 0.083 mol) and aniline (7.7 g, 0.083 mol) according to literature [33]. GPC: $M_n = 35\,000$, $M_w = 79\,000$, MWD = 2.2. IR (KBr): 3380 (O–H, m), 1600 1510 1463 (Benz. ring, s), 1250 cm^{-1} (C–O, s). ^{1}H NMR (DMSO-d_6): $\delta = 7.07$ (6H, d), 6.82 (4H, d), 6.72 (2H, d), 6.54 (1H, m), 4.03 (2H, m), 3.87 (4H, s), 3.34–3.75 (4H, m), 1.55 (6H, s).

DP–AN: 4,4′-Bis(2,3-epoxypropoxy)diphenyl (9.6 g, 0.032 mol) and aniline (2.7 g, 0.029 mol) were mixed and slowly heated. After melted, the mixture was kept at 110 °C for 48 h. The solid formed was dissolved in 100 ml DMF, and precipitated with plenty of water. The precipitate was dried and dissolved in 100 ml THF, then precipitated with petroleum ether. The solid was collected after vacuum drying at 70 °C for 24 h. GPC: $M_n = 14\,000$, $M_w = 30\,000$, MWD = 2.1. IR (KBr): 3357(O–H,m), 1604 1498 1460 (Benz. ring, s), 1242 cm^{-1} (C–O, s). ^{1}H NMR (DMSO-d_6): $\delta = 7.52$ (4H, d), 7.13 (2H, d), 7.00 (4H, d), 6.79 (2H, d), 6.57 (1H, m), 4.09 (2H, m), 3.97 (4H, s), 3.40–3.76 (4H, m).

PP–AN: Via a procedure similar to that described above for the synthesis of DP–AN. PP–AN was obtained from the reaction between 1,4-bis(2,3-epoxypropoxy)benzene and aniline. The product was dissolved in THF and precipitated with CCl_4. GPC: $M_n = 21\,000$, $M_w = 48\,000$, MWD = 2.3. IR (KBr): 3340 (O–H, m), 1600 1508 1460 (Benz. ring, s), 1232 cm^{-1} (C–O, s). ^{1}H NMR (DMSO-d_6): $\delta = 7.10$ (2H, d), 6.88 (4H, d), 6.75 (2H, d), 6.55 (1H, m), 4.04 (2H, m), 3.86 (4H, s), 3.40–3.75 (4H, m).

PP–AZ–NT: PP–AN (0.63 g, 2.0 mmol) was dissolved in DMF (66 ml) at 0 °C. A diazonium salt of 4-nitroaniline was prepared by adding an aqueous solution of sodium nitrite (0.199 g, 2.88 mmol in 0.6 ml of water) into a solution of 4-nitroaniline (0.331 g, 2.4 mmol)[1] in a homogeneous mixture of 0.6 ml of sulfuric acid and 6 ml of glacial acetic acid. The mixture was stirred at 0 °C for 1 min and then was added dropwise into the PP–AN solution. The solution was stirred at 0 °C for 12 h. Then the solution was poured into plenty of water and the precipitate was collected and dried. The product was dissolved in 40 ml THF and precipitated into 400 ml petroleum ether. The final product was vacuum dried at 70 °C for 24 h. IR (KBr): 3400 (O–H, m), 1600 1508 (Benz. ring, s), 1230 cm^{-1} (C–O, s). ^{1}H NMR (DMSO-d_6): $\delta = 8.31$ (2H, d), 7.89 (2H, d), 7.78 (2H, d), 6.92 (6H, d), 4.12 (2H, m), 3.80–4.00 (6H, br), 3.40–3.70 (2H, m).

All other azo polymers were synthesized by post-polymerization azo-coupling reactions. The diazonium salt preparations and coupling conditions are similar to that described above for the synthesis of PP–AZ–NT. Analytic results are given below.

PP–AZ–CA: IR (KBr): 3400 (O–H, m), 1700 (C=O, s), 1600 1508 (Benz. ring, s), 1230 cm^{-1} (C–O, s). ^{1}H NMR (DMSO-d_6): $\delta = 8.05$ (2H, d), 7.82–7.77 (4H, m), 6.92 (6H, d), 4.12 (2H, m), 3.80–4.00 (6H, br), 3.40–3.70 (2H, m).

PP–AZ–CN: IR (KBr): 3420 (O–H, m), 2225 ($\mathrm{C\equiv N}$, m), 1599 1506 (Benz. ring, s), 1230 cm^{-1} (C–O, s). ^{1}H NMR (DMSO-d_6): $\delta = 7.94$ (2H, d), 7.85 (2H, d), 7.77 (2H, d), 6.92 (6H, d), 4.12 (2H, m), 3.80–4.00 (6H, br), 3.40–3.70 (2H, m).

DP–AZ–NT: IR (KBr): 3420 (O–H, m), 1600 1500 (Benz. ring, s), 1240 cm^{-1} (C–O, s). ^{1}H NMR (DMSO-d_6): $\delta = 8.33$ (2H, d), 7.89 (2H, d), 7.80 (2H, d), 7.52 (4H, d), 7.01 (6H, d), 4.18 (2H, m), 3.90 (4H, s), 3.59–3.84 (4H, m).

DP–AZ–CA: IR (KBr): 3350 (O–H, m), 1706 (C=O, s), 1600 1510 (Benz. ring, s), 1245 cm^{-1} (C–O, s). ^{1}H NMR (DMSO-d_6): $\delta = 8.05$ (2H, d), 7.89 (4H, m), 7.51 (4H, d), 7.02 (6H, d), 4.18 (2H, m), 4.01 (4H, m), 3.59–3.89 (4H, m).

DP–AZ–CN: IR (KBr): 3400 (O–H, m), 2225 ($\mathrm{C\equiv N}$, m), 1600 1498 (Benz. ring, s), 1242 cm^{-1} (C–O, s). ^{1}H NMR (DMSO-d_6): $\delta = 7.95$ (2H, d), 7.85 (2H, d), 7.78 (2H, d), 7.53 (4H, d), 7.02 (6H, d), 4.18 (2H, m), 4.01 (4H, s), 3.50–3.90 (4H, m).

BP–AZ–NT: IR (KBr): 3420 (O–H, m), 1602 1510 (Benz. ring, s), 1243 cm^{-1} (C–O, s). ^{1}H NMR (DMSO-d_6): $\delta = 8.31$ (2H, d), 7.89 (2H, d), 7.76 (2H, d), 7.07 (4H, d), 6.91 (2H, d), 6.83 (4H, d), 4.11 (2H, m), 3.70–4.00 (6H, br), 3.40–3.65 (2H, m), 1.54 (6H, s).

BP–AZ–CA: IR (KBr): 3350 (O–H, m), 1700 (C=O, s), 1598 1508 1460 (Benz. ring, s), 1240 cm^{-1} (C–O, s). ^{1}H NMR (DMSO-d_6): $\delta = 8.05$ (2H, d), 7.80 (2H, d), 7.75 (2H, d), 7.08 (4H, d), 6.91 (2H, d), 6.84 (4H, d), 4.11 (2H, m), 3.70–4.00 (6H, br), 3.40–3.70 (2H, m), 1.54 (6H, s).

BP–AZ–CN: IR (KBr): 3430 (O–H, m), 2227 ($\mathrm{C\equiv N}$, m), 1599 1510 (Benz. ring, s), 1247 cm^{-1} (C–O, s). ^{1}H NMR (DMSO-d_6): $\delta = 7.93$ (2H, d), 7.84 (2H, d), 7.73 (2H, d), 7.07 (4H, d), 6.90 (2H,d), 6.83 (4H, d), 4.11 (2H, m), 3.70–4.00 (6H, br), 3.40–3.70 (2H, m), 1.54 (6H, s).

2.4. Polymer film preparation

The homogeneous solutions of polymers in anhydrous *N*, *N*′-dimethylformamide (DMF) were filtered through 0.45 μm membranes and spin-coated onto glass slides. The film thickness was controlled to be in the range of 1.0–1.6 μm by adjusting the solution concentration and the spin speed. The spin-coated films were dried at 60–70 °C under vacuum for 48 h and were stored in a desiccator for further measurements.

2.5. Surface-relief-grating fabrication

The experimental setup for the grating formation is similar to that reported in the literature [7,8]. A linearly polarized laser beam at 488 nm from an Ar^+ laser was used as a recording light source. The p-polarized laser beam was expanded and collimated. Half of the collimated beam was incident on the film directly and the other half of the beam was reflected onto the film from a mirror. The intensity of the recording beam was about 150 $\mathrm{mW/cm^2}$. The diffraction efficiency of the first order diffracted beam from the gratings in transmission mode was probed with an unpolarized low power He–Ne laser beam at 633 nm as described in the literature [8]. Even only weak absorption at wavelength of 633 nm, the absorption effect of the polymer films was corrected for calculating the diffraction efficiency.

3. Results and discussion

3.1. Polymer synthesis and characterization

Epoxy-based precursor polymers of three kinds were prepared through the step polymerization as shown in Scheme 1. Epoxide monomers diglycidyl ether of bisphenol-A, 1,4-bis(2,3-epoxypropoxy)benzene, and 4,4′-bis(2,3-epoxypropoxy)-diphenyl were reacted with aniline for preparing the epoxy-based precursor polymers, respectively. To avoid the reaction between the secondary OH groups formed during the polymerization and the unreacted epoxide groups, the polymerizations were carried out at a relatively low temperature (110 °C). All three precursor

---

[1] The amount depend on the required degree of functionalization. Only that for preparing polymers with approximate 100% DFs are given here.

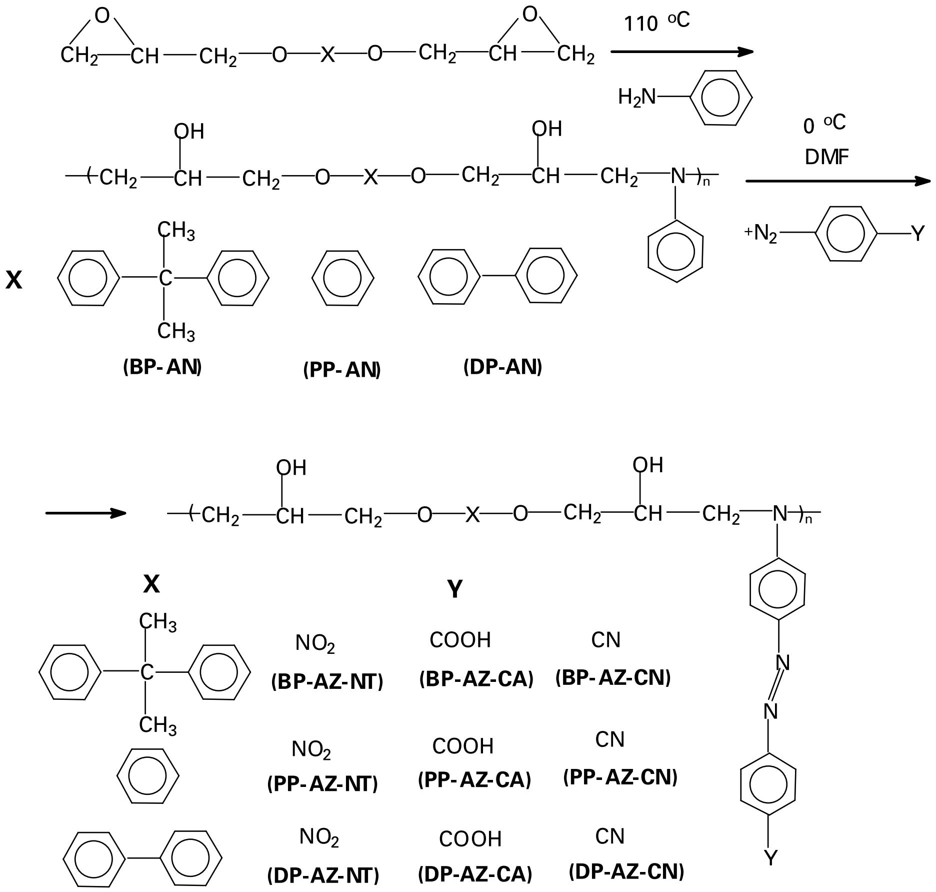

Scheme 1. Synthetic route of the epoxy-based azo polymers.

polymers are linear polymers with number-average molecular weights 35 000, 14 000, 21 000 and polydispersity indexes 2.2, 2.1, 2.3 for BP–AN, DP–AN, PP–AN determined by GPC, respectively. BP–AN and PP–AN are amorphous polymers with glass transition temperatures at 90 and 85 °C. DP–AN is a liquid crystal polymer with T_g, T_m, and T_i at 110, 126 and 185 °C. The polymers show good solubility in polar solvents such as DMF.

The precursor polymers were functionalized to introduce various azo chromophores through azo-coupling reaction at the final stages of the synthetic routes. The synthetic route and azo polymers synthesized in this work are shown in Scheme 1. The first part of the acronym names represent different precursor polymers and last parts denote electron-withdrawing groups –COOH, $-NO_2$, and –CN on the azobenzene units. For precursor polymers, the chemical shifts of unreacted aniline moieties appear at about 7.07 ppm (overlapped in BP–AN), 6.72 ppm (doublet), and 6.54 ppm (multiplet), attributed to the protons at *meta*, *ortho*, and *para* positions of the amino groups. When slight excesses of diazonium salts (molar ratios to aniline moieties of the precursor polymers) were used in all these reactions, the following changes in the ^1H NMR spectra were observed for aniline moieties in the precursor polymers upon post-polymerization azo-coupling reaction. The resonance (6.54 ppm) corresponding to the protons at *para* position of amino group disappeared. The chemical shifts of protons *ortho* and *meta* to the amino groups shifted to lower magnetic field, due to the presence of electron-withdrawing groups introduced by the azo-coupling reaction and the increase of the conjugation length. Moreover, additional resonances corresponding to chemical shifts of the benzenoid ring protons introduced through the post-polymerization azo-coupling reaction appeared at a lower magnetic field. It could be concluded that the azo-coupling reactions occur at the *para* positions of aniline moieties with high yields for all the epoxy-based precursor polymers reported in this work. From the ^1H NMR spectra, the DFs were estimated to be almost 100%.

3.2. Degree of functionalization

By the post-polymerization azo-coupling scheme, the degrees of functionalization (DFs) of the azo polymers can be easily adjusted by selecting suitable feed ratios. In this study, the feed ratios are defined as the molar ratios between the diazonium salts and the aniline moieties of the precursor polymers. DFs of the azo polymers were determined by ^1H NMR analysis. For instance of the BP–AN series of the polymers, the DFs were estimated from ^1H NMR by

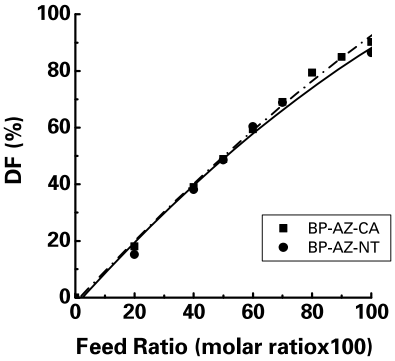

Fig. 1. Relationship between the DFs and the feed ratios for BP–AZ–CA and BP–AZ–NT.

comparing the peak areas for the protons *meta* to the amino groups in substituted aniline moieties with the peak areas at 1.55 ppm corresponding to the methyl protons of the bisphenol-A moieties.

The relationships between the molar feed ratios and the DFs for two series of azo polymers are shown in Fig. 1. When the feed ratios were lower than 50%, the DFs increased linearly with the feed ratios. The added diazonium salts almost completely reacted with the aniline moieties of the precursor polymers. When the feed ratios were higher than 50%, the DFs were slightly lower than the feed ratios. It can be explained that the increased steric hindrance at reaction sites resulted from the increased amount of the bulky azobenzene groups on the polymer chains. When the degree of functionalization was high, it became more difficult for diazonium salt molecules to reach the reaction sites. Some side reactions, undesirably consuming a part of the diazonium salts, had occurred before the azo-coupling reaction could take place. Therefore, in this range, slightly excessive amounts of diazonium salts were required to obtain the designed DFs.

3.3. Thermal and spectral properties

The azo polymers, with different kinds of backbones and azo chromophores, all showed thermal behavior of typical amorphous polymers. The T_gs of polymers estimated from DSC measurements are given in Table 1. Precursor polymer DP–AN is a liquid crystal polymer, but all DP–AN based azo polymers obtained from the post-functionalization no longer show any mesophase behavior. It is due to the introduction of the bulky azo chromophores, which interrupt the tight and anisotropic packing of the polymer chains.

Table 1
T_gs of the prepared epoxy-based azo polymers

Precursor polymers	T_gs (°C) of azo polymers		
	NO_2[a]	CN[a]	COOH[a]
BP–AN	138	132	160
DP–AN	134	134	155
PP–AN	131	130	143

[a] Substituents at 4-positions of azobenzene units.

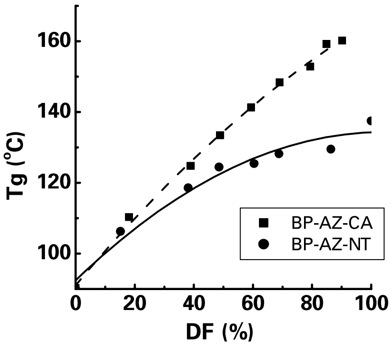

Fig. 2. Relationship between the glass transition temperatures and the DFs for BP–AZ–CA and BP–AZ–NT.

For each type of the backbone, the glass transition temperatures (T_gs) of the fully functionalized azo polymers were observed to be much higher than that of the corresponding precursor polymer due to the significant increases in both the size and the polarity of the side groups (Table 1). For the same precursor polymer, the polymer containing 4-carboxylazobenzene chromophores showed a considerably higher T_g than that of the polymer containing 4-nitroazobenzene or 4-cyanoazobenzene chromophores (Table 1), which can be attributed to the hydrogen bonding between COOH groups. For the azo polymers with the same types of backbones and azo chromophores, the T_gs of the polymers depended on the DFs. The relationships between the T_gs and the DFs for two series of the azo polymers are shown in Fig. 2. For BP–AZ–NT, the T_g of the azo polymer increased with the DF increase because of the growing loading density of the rigid and polar side groups. When the DF was high, the bulky side groups could also prohibit the tight packing between the polymer chains. The further increase of polymer T_g with the DF became less significant at the range of high DF. On the contrary, the T_g of the BP–AZ–CA increased almost linearly with the DF increase until DF reached 100%. It is believed that the linearly increasing relationship between T_g and DF for BP–AZ–CA is also related with the hydrogen bondings existed in the system.

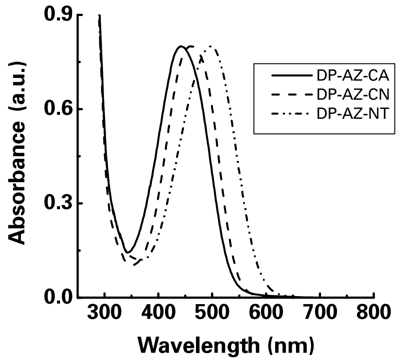

Fig. 3. UV–vis spectra of the DP–AN based azo polymers in DMF.

Table 2
λ_{max}s of the azo polymers in DMF solutions or as spin-coated films

Precursor polymers	λ_{max} (nm) of azo polymers (DMF solutions/spin-coated films)		
	NO_2[a]	CN[a]	COOH[a]
BP–AN	498/482	460/449	445/431
DP–AN	498/482	460/450	442/435
PP–AN	496/482	466/450	443/434

[a] Substituents at 4-positions of the azobenzene units.

The UV–vis spectra of the DP–AN based azo polymers in DMF solutions are shown in Fig. 3. The curves show typical absorption behavior of the pseudo-stilbene type of azo chromophores, e.g. bands corresponding to the $\pi-\pi^*$ transition appear at longest wavelength and chromophores exhibit strong absorption in the visible region [5]. The UV–vis spectra of the BP–AN and PP–AN based azo polymers in DMF solutions are similar with those of DP–AN based azo polymers. As expected, the λ_{max}s were observed to be strongly affected by the *para*-substituents of the azo chromophores due to their inductive and conjugative effect on both the ground and excited states. λ_{max}s of the azo polymers in DMF solutions and as spin-coated films are given in Table 2. The λ_{max}s of the epoxy-based azo polymers as spin-coated films showed significant blue-shifts as compared with those of the azo polymers containing the same types of azo chromophores in DMF solutions.

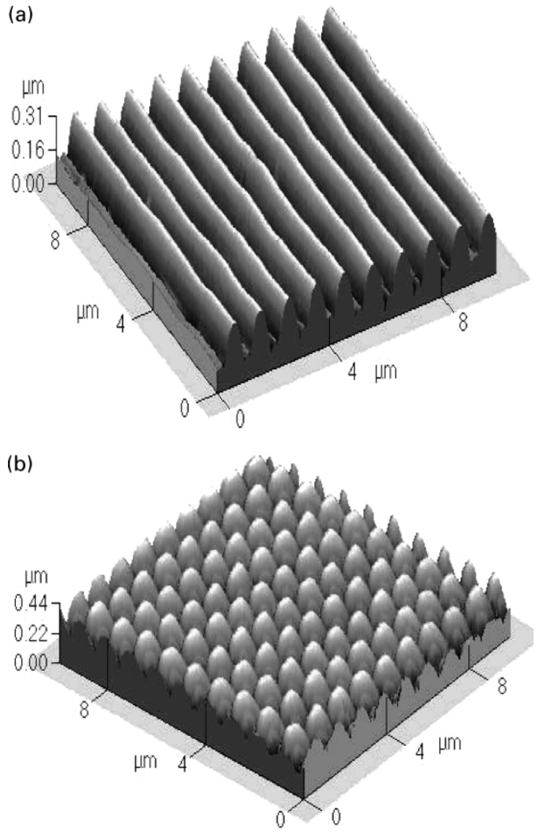

Fig. 4. AFM images of the SRGs formed on DP–AZ–CN films: (a) 3D view of the SRG, (b) orthogonal gratings.

3.4. Photoinduced surface-relief-gratings

The surface-relief-grating (SRG) formation process was studied for the spin-coated thin films of the epoxy-based azo polymers. The experimental setup was similar to that reported by other groups and described in Section 2 [7,8]. The interference pattern of Ar^+ laser beams was produced by two p-polarized beams. Although, the p/p-polarization condition is not as efficient as conditions such as using two circularly polarized interfering beams (left-circularly polarized: right-circularly polarized), the condition can produce good quality SRG and the result is relatively easy to be explained [22–25]. All the azo polymers prepared in this work could form typical SRGs upon exposure to an interference pattern of Ar^+ laser beams at modest intensities. Fig. 4(a) shows atomic force microscopy (AFM) image of the sinusoidal surface relief structures with regular spaces formed on the DP–AZ–CN film. The spatial period depends on the wavelength λ of the writing beam and the angle θ between the two interfering beams, which has a relationship as [22]

$$\Lambda = \lambda/2\sin(\theta/2)$$

Fig. 4(b) shows the AFM images of the surface relief structures when two gratings are recorded orthogonally to each other at the same location. The depths of the gratings formed in typical cases were in the range from 100 to 250 nm.

SRG forming behavior of the synthesized azo polymers was characterized by the inscription rates and the saturation levels of SRG formation. The first order diffraction efficiency of the SRGs recorded in situ was used to characterize the surface modification [12–15]. The results were also compared with the surface deformation obtained from the AFM images. Low power Ar^+ (<150 mW/cm^2) was used for the writing experiments in order to avoid the possible side effect caused by high intensity laser

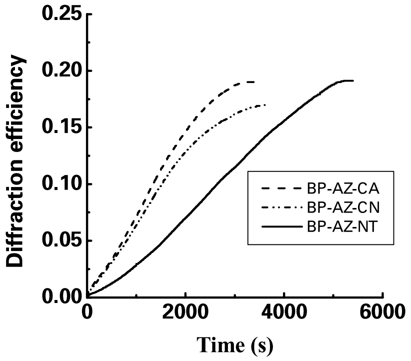

Fig. 5. Diffraction efficiency as a function of the irradiation time for azo polymers BP–AZ–CA, BP–AZ–CN and BP–AZ–NT.

irradiation. For comparative experiments, the laser powers were controlled to be the same for each experiment. It has been reported that the dependence of inscription rates on the film thickness can be ignored for relatively thick (>0.5 μm) films [32]. Therefore, films with thicknesses greater than 1 μm were used in this work and the thickness of films used for comparative experiments were all controlled to be approximately the same.

Fig. 5 shows the diffraction efficiency as a function of irradiation time for three epoxy-based azo polymers containing different azo chromophores with DFs of approximate 100%. The azo polymers BP–AZ–CA, BP–AZ–CN and BP–AZ–NT, which are distinguished only by electron-withdrawing groups of the azo chromophores, showed significantly different inscription rates of SRG formation. With the same backbone, the polymer containing 4-nitroazobenzene chromophores and 4-carboxyazobenzene were found to exhibit the slowest and fastest inscription rates for SRG formation among the three polymers. The increases of the diffraction efficiency of the SRGs with irradiation time were saturated for BP–AZ–CA, BP–AZ–CN and BP–AZ–NT at 3000, 3300 and 5000 s, respectively. The saturation levels for BP–AZ–CA and BP–AZ–NT were almost the same. The saturation level for BP–AZ–CN was about 2% lower. The λ_{max} of BP–AZ–NT is in range 482–483 nm, which is nearest to the 488 nm irradiation of the Ar^+ laser. However, the SRG forming rate was observed to be obviously slower than the rate of BP–AZ–CA or BP–AZ–CN bearing 4-cyanoazobenzene or 4-carboxyazobenzene chromophores (λ_{max}s at 449–450 or 431–435 nm). This observation contradicts the simple deduction that irradiation at λ_{max} could accelerate the *trans–cis–trans* circles and increase the inscription rates. The reason for this result is still unclear to us at present stage.

Above results suggest that the substituents at 4-positions of the azobenzene units have a significant influence on the inscription rate of SRG formation. The similar influence was also observed for the other epoxy-based azo polymers prepared in this work. To our knowledge, no directly comparable results are available in published literatures. Barrett et al. have studied the substituent effect by comparing three azo chromophores with different van der Waals occupied volumes. It has been found that an increase in free volume required for the photoreaction results in the increased inscription rate [12]. Three types of azo chromophores studied in this work do not have substantial difference in the occupied volume. To explain this type of substituent effect, the inductive and conjugative effects of substituents on photoresponsive behavior of the azo chromophores themselves need to be considered. Helgert et al. have demonstrated that the substituents on azobenzene units have an effect to determine whether the peaks or valleys are formed in the illuminated areas. The irradiation intensity (1–6 W/cm^2) reported in Helgert's work is much higher than that used in this work. It has been reported that high-intensity irradiance effect may create a SRG on polymer films through a different mechanism [24,27]. Therefore, it should be extremely cautious to compare data produced with significantly different irradiation intensity.

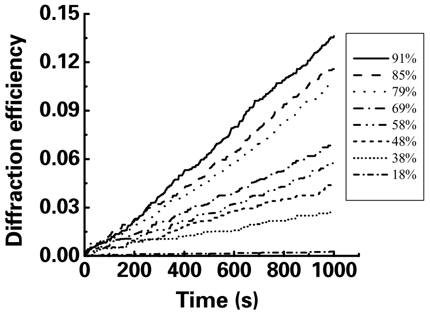

Fig. 6. Diffraction efficiency as a function of the irradiation time for BP–AZ–CA with the different degrees of funtionalization.

Fig. 6 shows the diffraction efficiency as a function of the irradiation time for BP–AZ–CA with different DFs. For each DF, the increase of the diffraction efficiency with irradiation time shows different rate. Fig. 7 shows the relationship between the surface modulation and the degree of functionalization for the same series of polymers characterized by both the diffraction efficiency measurement and AFM. Both results show that the surface modulations at the same irradiation time increase with the

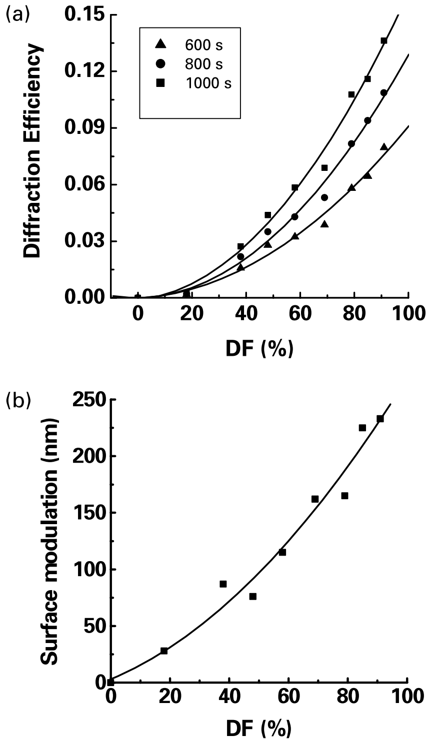

Fig. 7. Relationship between surface modulation and degree of functionalization for BP–AZ–CA: (a) measured from the diffraction efficiency experiments at 600, 800, and 1000 s; (b) measured from AFM images after 1000 s irradiation.

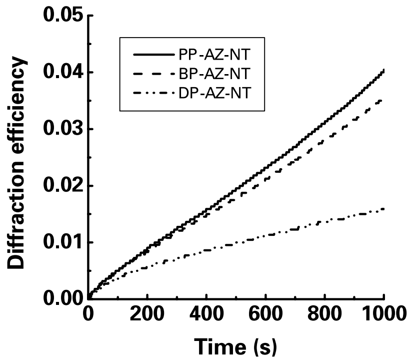

Fig. 8. Diffraction efficiency as a function of the irradiation time for three epoxy-based azo polymers, with the same type of azo chromophores and different types of backbones.

increased amount of azobenzene chromophores attached to each polymeric chain. Fukuda et al. has reported that the SRG formation rate exhibited an S-shaped dependence on the azo functionalization. Above 40–50 wt% degree of functionalization, the inscription rate was independent of the degree of functionalization [32]. In this study, the DFs for fully functionalized epoxy-based polymers, defined as the molar ratio of the functionalized aniline moieties to total aniline moieties, were lower than the saturation point reported by Fukuda.

The effect of the backbones on the inscription rates of the azo polymers were observed by comparing the SRG forming rates of the azo polymers with the same type of chromophores and different type of backbones (Fig. 8). Although the type of azo chromophores and the way they are attached to the backbones were the same, the inscription rates of PP–AZ–NT, DP–AZ–NT, and BP–AZ–NT were observed to be obviously different. PP–AZ–NT exhibited the fastest inscription rate and BP–AZ–NT had a slightly slower rate, while DP–AZ–NT possessed the slowest inscription rate. The fastest inscription rate of PP–AZ–NT could be attributed to the highest chromophore loading density among the three polymers. The slower rate of DP–AZ–NT compared with BP–AZ–NT could be attributed to the backbone rigidity of DP–AZ–NT that affected the effective viscosity of the system.

4. Conclusions

Three kinds of epoxy-based precursor polymers have been post-functionalized to introduce different types of azo chromophores with selected DFs. The SRGs on the polymer films were photofabricated by using interferenced Ar^+ laser beams. SRGs with large surface modulation were observed on all the azo polymer films. The inscription rates of the azo polymers depended on the substituents of the azobenzene units, the DFs and the types of backbones. For the polymers studied in this work, the azo polymers containing 4-nitroazobenzene chromophores showed significantly slower rates for the surface deformation than the azo polymers bearing 4-cyanoazobenzene or 4-carboxyazobenzene chromophores. The SRG inscription rates increased with the degree of functionalization for the epoxy-based polymers. The study on the epoxy-based polymers bearing the same types of azo chromophores revealed that the polymer with a more flexible main-chain or high chromophore loading density showed a faster SRG forming rate. These results suggest that the azo chromophores in the polymers play a key role in the SRG forming process. Meanwhile, the backbone structure also has some influences on the process.

Acknowledgements

Funding from project 59873013 supported by NSFC is gratefully acknowledged.

References

[1] Todorov T, Nikolova L, Tomova A. Appl Opt 1984;23:4588.
[2] Eich M, Wendroff JH, Reck B, Ringsdorf H. Makromol Chem Rapid Commun 1987;8:59.
[3] Kumar GS, Neckers DC. Chem Rev 1989;89:1915.
[4] Kumar GS. Azo functional polymers: functional group approach in macromolecular design. Lancaster: Technomic Publishing Company Inc; 1993.
[5] Rau H. In: Rabek JF, editor. Photochemistry and photophysics, vol. II. Boca Raton, FL: CRC Press; 1990.
[6] Xie S, Natansohn A, Rochon P. Chem Mater 1993;5:403.
[7] Rochon P, Batalla E, Natansohn A. Appl Phys Lett 1995;66:136.
[8] Kim DY, Tripathy SK, Li L, Kumar J. Appl Phys Lett 1995;66:1166.
[9] Ramanujam PS, Holme NCR, Hvilsted S. Appl Phys Lett 1996;68:1329.
[10] Kim DY, Li L, Jiang XL, Shivshankar V, Kumar J, Tripathy SK. Macromolecules 1995;28:8835.
[11] Jiang XL, Li L, Kim DY, Shivshankar V, Kumar J, Tripathy SK. Appl Phys Lett 1996;68:2618.
[12] Barrett C, Natansohn A, Rochon P. J Phys Chem 1996;100:8836.
[13] Ho MS, Barrett C, Paterson J, Esteghamatian M, Natansohn A, Rochon P. Macromolecules 1996;29:4613.
[14] Jiang XL, Li L, Kumar J, Kim DY, Tripathy SK. Appl Phys Lett 1998;72:2502.
[15] Tripathy SK, Kim DY, Li L, Kumar J. Chemtech 1998;28:34.
[16] Viswanathan NK, Kim DY, Bian S, Williams J, Liu W, Li L, Samuelson L, Kumar J, Tripathy SK. J Mater Chem 1999;9:1941.
[17] Kipfer P, Collischon M, Haidner H, Schwider J. Opt Engng 1996;35:726.
[18] Liu J, Azzam RMA. Appl Opt 1996;35:5557.
[19] Barratt CJ, Rochon P, Natansohn A. J Chem Phys 1998;109:1505.
[20] Pedersen TG, Johansen PM, Holme NCR, Ramanujam PS, Hilvsted S. Phys Rev Lett 1998;80:89.
[21] Lefin P, Fiorini C, Nunzi JM. Pure Appl Opt 1998;7:71.
[22] Kumar J, Li L, Jiang XL, Kim DY, Lee TS, Tripathy SK. Appl Phys Lett 1998;72:2096.
[23] Viswanathan NK, Balasubramanian S, Li L, Tripathy SK, Kumar J. Jpn J Appl Phys 1999;38:5928.
[24] Bian S, Williams JM, Kim DY, Li L, Balasubramanian S, Kumar J, Tripathy SK. J Appl Phys 1999;86:4498.
[25] Bian S, Li L, Kumar J, Kim DY, Williams J, Tripathy SK. Appl Phys Lett 1998;73:1817.

[26] Helgert M, Wenke L, Hvilsted S, Ramanujam PS. Appl Phys B 2001;72:429.

[27] Rasmussen PH, Ramanujam PS, Hvilsted S, Berg RH. J Am Chem Soc 1999;121:4738.

[28] Sukwattanasinitt M, Wang XG, Li L, Jiang XL, Kumar J, Tripathy SK, Sandman DJ. Chem Mater 1998;10:27.

[29] Wang XG, Balasubramanian S, Kumar J, Tripathy SK, Li L. Chem Mater 1998;10:1546.

[30] Lee TS, Kim DY, Jiang XL, Kumar J, Tripathy SK. J Polym Sci, Part A 1998;36:283.

[31] Xu Z, Drnoyan V, Natansohn A, Rochon P. J Polym Sci, Part A 2000;38:2245.

[32] Fukuda T, Matsuda H, Shiraga T, Kimura T, Kato M, Viswanathan N, Kumar J, Tripathy SK. Macromolecules 2000;33:4220.

[33] Wang XG, Chen J, Marturunkakul S, Li L, Kumar J, Tripathy SK. Chem Mater 1997;9:45.

[34] Wang XG, Kumar J, Tripathy SK, Li L, Chen J, Marturunkakul S. Macromolecules 1997;30:219.

[35] Carfagan C, Amendola E, Giamberini M, Hakemi H, Pane S. Polym Int 1997;44:465.